

Stimulation of static deconfined medium by multiple hard partons

Martin Schulc¹ and Boris Tomášik^{1,2}

¹Czech Technical University in Prague, FNSPE, 11519 Prague, Czech Republic

²Univerzita Mateja Bela, 97401 Banská Bystrica, Slovakia

E-mail: `boris.tomasik@umb.sk`

Abstract. We investigate the response of non-expanding deconfined hot matter to energy and momentum deposition from a pair of partons moving with high energies. Several situations are examined with partons moving so that the generated wakes in the medium interact. The resulting energy and flow profiles are studied. Such cases are relevant for nuclear collisions at the LHC where several hard partons are produced in a single collision and their contribution to collective expansion of the fireball may be important.

PACS numbers: 25.75.-q, 25.75.Ld

1. Introduction

Nuclear collisions prepared at the Large Hadron Collider possess several unique features. Apart from the highest energy density ever obtained in a lab the initial state of the hot and dense strongly interacting medium includes a number of hard partons. For example, in a central Pb+Pb collision at full LHC energy of 5.5 A TeV one expects on average more than 8 hard partons with transverse energy above 20 GeV within central 5 units of pseudorapidity [1]. This number grows exponentially if we decrease the required energy of the jets.

Such hard partons deposit a large part (if not all) of their energy and momentum into the thermalised medium. This leads to lumps of energy and momentum density in the hot matter. Currently, much attention is devoted to such lumps in the energy density—called sometimes hot spots—which appear in the initial state for the hydrodynamical expansion [2, 3, 4, 5, 6, 7, 8, 9, 10, 11]. These initial state inhomogeneities are being linked with the measured azimuthal anisotropies of hadron distributions [12]. In this paper, however, we focus our attention to energy and momentum deposition from hard partons [13, 14, 15] which goes beyond the hot spots picture in at least two aspects: Firstly, momentum transferred to the medium has a direction in contrast to the energy density making up a hot spot. Secondly, it is being deposited over some period of time and not just instantaneously at the beginning of the expansion. Technically, this means that energy and momentum deposition from

hard partons are not treated as an initial condition for the hydrodynamic expansion but rather through a source term of the hydrodynamic equations.

Azimuths of the hard partons are distributed symmetrically. Nevertheless, their numbers in individual collisions are not large and thus on event-by-event basis one might naturally expect anisotropies in the transverse flow. They are naturally expressed through higher order terms in the harmonic expansion in the azimuthal particle distribution. When summed over a large number of events one would first expect any anisotropies in particle production to even out due to original isotropy of hard parton production. It has been, however, argued that due to collective response of the hydrodynamic medium an asymmetry of the transverse expansion might be generated in the fireball that leads to quadrupole anisotropy in hadron production [16]. In that paper, however, the argument was supported only by a toy model simulation without really modelling the hydrodynamic response to the hard partons.

It has been studied by several authors by now how the medium responds to energy and momentum deposition from one hard parton [13, 14, 15, 17, 18, 19, 20, 21, 22, 23, 24, 25]. It has been also shown [13] that the generated wake continues to travel even after the hard parton lost all of its energy and thermalised in the medium. In this paper we investigate how the excitations of the hot matter continue to evolve in case there are two of them generated. We confirm the ansatz made in the toy model [16] that two wakes merge when they approach each other and continue to stream united according to energy and momentum conservation. This validates the conclusions made in that paper that the effect contributes to the elliptic flow.

The rest of the paper is divided into three sections: First we introduce the hydrodynamic model that was used in our simulations. In Section 3 we present results obtained with this model for simulations of energy and momentum deposition from pairs of jets in different configurations. Our findings are summarised in Section 4.

2. The hydrodynamic model

The relativistic hydrodynamic equations express the conservation of energy, momentum, and baryon number:

$$\partial_\mu T^{\mu\nu}(x) = J^\nu, \quad (1)$$

$$\partial_\mu J_B^\mu(x) = 0, \quad (2)$$

where $T^{\mu\nu}(x)$ is the energy-momentum tensor and $J_B^\mu(x)$ is the baryon current. The source current J^ν will be discussed below. In the case of relativistic ideal fluid, the energy-momentum tensor and baryon current are given by

$$T^{\mu\nu} = (\epsilon + p)u^\mu u^\nu - pg^{\mu\nu}, \quad (3)$$

$$J_B^\mu(x) = n_B(x)u^\mu(x), \quad (4)$$

where $\epsilon(x)$, $p(x)$, $n_B(x)$, and $u^\mu = \gamma(1, \vec{v})$ are the proper energy density, pressure and baryon density which are evaluated in the rest frame of the fluid, and flow four-velocity,

respectively. The factor $\gamma = (1 - \bar{v}^2)^{-\frac{1}{2}}$. We set the net baryon density to zero in this study and consider medium without collective velocity field generated by pressure. The system of equations (1) is closed by specifying the equation of state $p = p(\epsilon)$. In our study, we will employ the equation of state by Laine and Schroder [26], which is derived from high-order weak-coupling perturbative QCD calculation at high temperatures, a hadron resonance gas at low temperatures, and an analytic interpolation in the crossover region between the high and low temperatures.

The term J^ν on the right-hand side of eq. (1) is the source term of energy-momentum conservation. It parametrises the deposition energy and momentum into the medium[‡]. In our study it will represent deposition from hard partons which are precursors of the jets. We will loosely call them jets although they have not yet built up their showers. The form of source term which describes the interaction of the jet with QGP is not known yet exactly, though some groups made progress on this topic [22, 25, 27, 28, 29, 30, 31]. In covariant notation it is given by [13]

$$J^\nu(x) = \sum_i \int_{\tau_{i,i}}^{\tau_{f,i}} d\tau \frac{dP_i^\nu}{d\tau} \delta^4(x^\mu - x_{jet,i}^\mu), \quad (5)$$

where $\tau_{f,i} - \tau_{i,i}$ denotes the proper time interval associated with the evolution of the i -th hard parton, $\vec{x}_{jet,i}$ describes its position, and $dP_i^\nu/d\tau$ is its energy-momentum loss rate along its trajectory $x_{jet,i}^\mu(\tau) = x_{0,i}^\mu + u_{jet,i}^\mu \tau$. Summation runs over all hard partons in the system. In practical simulation it is assumed that the jet deposits its energy and momentum over some region characterised by a Gaussian profile. Then, in non-covariant notation, the source term that we use is

$$J^\nu(x) = \sum_i \frac{1}{(\sqrt{2\pi}\sigma)^3} \exp\left(-\frac{[\vec{x} - \vec{x}_{jet,i}(t)]^2}{2\sigma^2}\right) \left(\frac{dE_i}{dt}, \frac{d\vec{P}_i}{dt}\right), \quad (6)$$

where it is chosen that $\sigma = 0.3$ fm. Energy deposition and momentum deposition in the direction of the moving jet are denoted dE/dt and dP/dt , respectively. The system with jets evolves in time until the simulation is stopped. The energy loss is modelled according to simplified Bethe-Bloch prescription [32] with an explosive burst of energy and momentum known as the Bragg peak [33]. Due to its interaction with the plasma, the jet will decelerate and its energy and momentum loss will change. The hard partons deposit energy and also momentum in the direction of their motion. The momentum loss is given as

$$\frac{dP}{dx} = \frac{1}{v_{jet}} \frac{dE}{dx} = a \frac{1}{v_{jet}^2}, \quad (7)$$

where v_{jet} is the jet velocity and a determines the absolute scale of the jet stopping. This equation shows that when the jet decelerates, the energy-momentum deposition

[‡] With the same term one can describe extraction of energy and momentum from the medium, but this case is not relevant and thus not elaborated here.

increases and has a peak for $v_{jet} \rightarrow 0$. In order to determine the actual velocity of the jet one can introduce jet rapidity

$$y_{jet} = \frac{1}{2} \ln \frac{1 + v_{jet}}{1 - v_{jet}}, \quad (8)$$

and then use the ansatz (7) and the identity $dP/dy_{jet} = m \cosh y_{jet}$, to derive the dependence of the time on the jet rapidity [13]

$$t(y_{jet}) = \frac{m}{a} \left[\sinh y_{jet} - \sinh y_0 - \arccos \frac{1}{\cosh y_{jet}} + \arccos \frac{1}{\cosh y_0} \right], \quad (9)$$

where y_0 is the initial rapidity of the jet. For all simulations the initial velocity was set to $v_0 = 0.9999$, the mass of the moving parton is assumed to be of the order of the constituent quark mass and was set to $m = 0.3$ GeV. The initial energy loss rate was usually set to $a = -4.148$ GeV/fm (unless stated otherwise). This value was determined from the fact that in our simulation jet stops after $\Delta\tau = 5.0$ fm/ c . The unperturbed static energy density of the medium was adjusted to $\epsilon_0 = 20.0$ GeV/fm³. The main difference between the ansatz described here and the Bethe-Bloch equation is that the momentum deposition is longitudinal rather than transverse.

For hydrodynamic simulation we use SHASTA algorithm [34] together with a multidimensional flux-correction [35] which is an improved version of Zalesak's method [36], to solve the (3+1)-dimensional system of hydrodynamic equations with source terms, e.g. eq. (1).

3. Results

We examine various types of static medium responses to perturbation by moving jets. In order to compare our results to [13] we begin with excitation of QGP by one hard parton moving along the x -axis. In [13] this situation was simulated for lower energy densities and energy deposition. Our values are more relevant for quark matter produced at the LHC while that paper was focussed more at RHIC§. The difference is also in the implemented equation of state: we use the QCD parametrisation of [26] instead of the relativistic ideal gas equation of state.

In the one jet scenario, hard parton deposits energy and momentum into static medium. Profiles of the energy density are shown in Fig. 1; the hard parton enters from left. The figure displays a sequence of energy density profiles during hydrodynamical evolution. We observe a spot with higher energy density at the position where jet deposits energy. The increase of the energy density spreads in a Mach-cone-like structure. Behind the jet there remains a wake with a dip in the energy density profile. The energy spreads even after the jet is fully stopped. Equivalent simulation using the ultrarelativistic equation of state ($\epsilon = 3p$) leads to no significantly different results. Typical energy densities in the simulation are far above the transition from hadrons to

§ In [13] the authors used energy-momentum deposition $dE/dx = 1.5$ GeV/fm and static quark gluon plasma with temperature $T_0 = 200$ MeV.

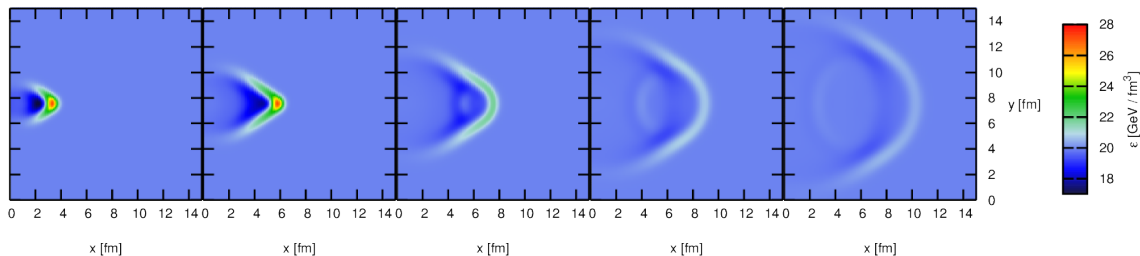


Figure 1. Sequence of energy density profiles during hydrodynamic evolution. One hard parton deposits energy and momentum into static medium. It enters from the left. First profile is taken after time delay $t = 2.5$ fm/ c . Each of the following profiles is taken with a delay $\Delta t = 2.5$ fm/ c after the previous profile. The energy of the parton is fully exhausted after 5 fm/ c . The initial energy loss is $dE/dx = -4.148$ GeV/fm, initial velocity of the parton is $v_{jet} = 0.9999$, and unperturbed static energy density is $\epsilon_0 = 20$ GeV/fm³.

quarks, where the sensitivity to different equations of state is strongest. Finally, the evolution of the jet is in qualitative agreement with results presented in [13]. Especially, the explosive burst of energy and momentum deposited by the jet immediately before it is fully quenched does not stop the strong flow behind the jet (the diffusion wake).

We check that the deposited momentum is almost fully contained in the wake. This is done by dividing the space into three regions: (I) is the tube with diameter 1.5 fm around the jet trajectory up to the shock front of the Mach wave, (II) is the rest of the matter behind the cone, and (III) is the region ahead of the shock front which is unaware of any energy deposition as yet. At the moment of jet extinction region (I) contains 92% of all jet momentum. After next 2.5 fm/ c this drops just a little to 87%. The rest of the momentum is diffused into region (II). This demonstrates our claim that deposited momentum shows up in form of streams of the hot medium.

Next, we show results for various scenarios including two hard partons. Figure 2 shows hydrodynamic evolution stimulated by two hard partons moving in opposite directions against each other. Both lose the same amount of energy. All energy is deposited into plasma before the two partons would meet at $t = 5$ fm/ c . At this time their distance is 3 fm. Hence, only the diffusion wakes meet and the two streams of plasma hit each other. The cone structures from both hard partons evolve like in previous case with just one hard parton. The two streams generated in the wakes meet and stop.

We also examine a setup with a pair of jets in the same directions as before but one of them deposits just one half of the energy of the other (Fig. 3). In total, the jet coming from the left side deposits 21.5 GeV of energy and the opposite one 10.5 GeV. Again, the Mach cones pass through each other and continue in their evolution. In Fig. 4 we see that the streams in the wakes continue after the jets are extinct and meet slightly closer to the extinction place of the less energetic jet due to different velocities. The

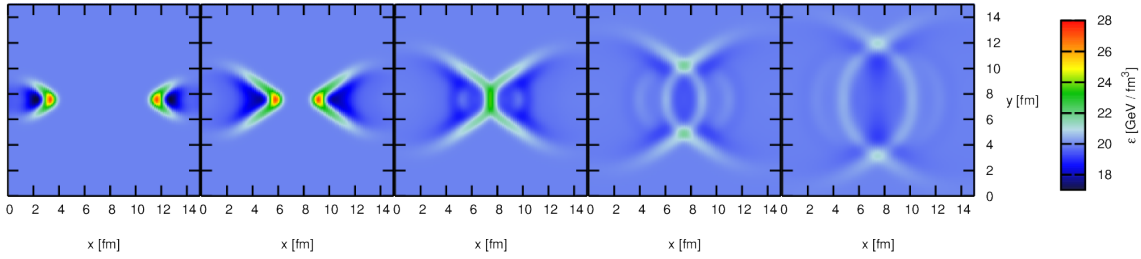


Figure 2. Sequence of energy density profiles during hydrodynamical evolution. Two hard partons deposit energy and momentum into static medium. They enter from the left and from the right and move against each other. The first profile is taken after time delay $t = 2.5$ fm/c. Following profiles are taken with subsequent delays of $\Delta t = 2.5$ fm/c. Partons are fully stopped after 5 fm/c. Initial energy loss is $dE/dx = -4.148$ GeV/fm, initial velocities are $v_{jet} = 0.9999$, and unperturbed static energy density is $\epsilon_0 = 20$ GeV/fm³.

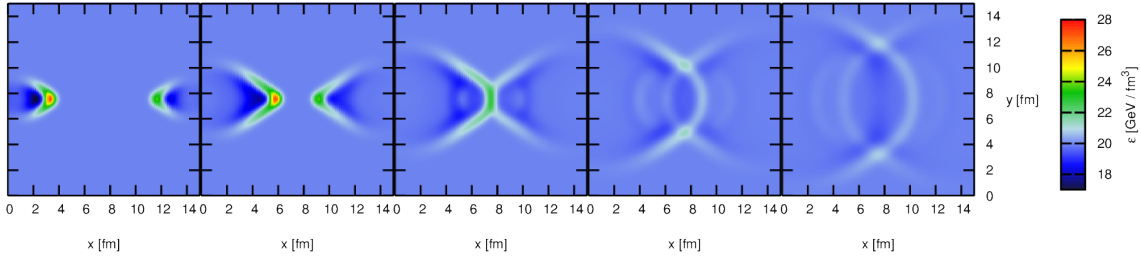


Figure 3. Sequence of energy density profiles during hydrodynamic evolution. Two hard partons deposit energy and momentum into static medium. They enter from the left and from the right and move against each other. First profile is taken after time delay $t = 2.5$ fm/c and following profiles after subsequent delays $\Delta t = 2.5$ fm/c. Jets are fully quenched after 5 fm/c. Initial energy loss of the left jet is $dE/dx = -4.148$ GeV/fm. The jet on the right loses one half of the energy of the other jet. The initial velocity of the jets is $v_{jet} = 0.9999$. Unperturbed static energy density is $\epsilon_0 = 20$ GeV/fm³.

more energetic streaming, however, does not overturn the streaming on the other side. Deposited momentum for various scenarios with jets aiming in opposite directions is also shown in Fig. 5. This figure confirms that the momentum density does not overrun to the other side even if one jet deposits more momentum than the other (blue dashed line). If the two jets do not collide exactly head-on, momentum density along the line between their trajectories shows the vortex structures [13]: close to the position of the parton there is momentum in the direction of the parton and shortly after it momentum turns into the other direction. This is the vortex where matter flows backwards from the Mach cone to the wake where the energy density and pressure is lower than in the unperturbed medium.

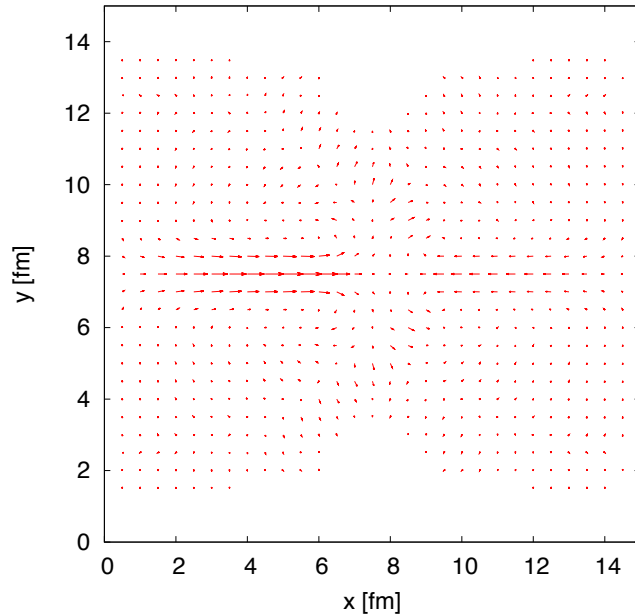


Figure 4. Momentum density profile resulting from the situation in Fig. 3. This profile is taken 10 fm/c after the start of the evolution, i.e. 5 fm/c after the jets are extinct. The length of the arrows is proportional to the local momentum density and their direction shows the direction of the momentum.

In real situation, jet-induced streams will come together under various angles. In order to see how they may interact we examine a situation where the two jets move perpendicularly. In Fig. 6 two hard partons—one entering from the left and one from the bottom in the same plane—deposit energy and momentum into static medium. The unperturbed momentum density here is again $\epsilon_0 = 20 \text{ GeV}/\text{fm}^3$. In order to see a stronger effect on the medium, energy-momentum deposition was doubled in comparison with previous examples, e.g. $dE/dx = -8.296 \text{ GeV}/\text{fm}$. Jets are fully stopped 1.5 fm/c before they would meet. We see that the conical structures of higher energy density look like a superposition of the two Mach cones that propagate also after the full quenching of the jets. In order to study the induced streaming of matter we plot the evolution of momentum density profile in Fig. 7. We can observe the merging of the two wake streams in the place where they come together. If energy-momentum deposition of the jet into medium is sufficient, on a small distance—until the energy is diffused too much—the streams continue together diagonally. Vortex-like structure in momentum density vectors in medium is present [13].

The merging of diffusion wakes is also demonstrated in Fig. 8. The figures display momentum density in the direction diagonal to the two jets as a function of the diagonal coordinate for various perpendicular jets scenarios. Left panel displays the situation when the wakes just merge ($t = 7.5 \text{ fm}/c$). Right panel shows the situation after another 2.5 fm/c ($t = 10.0 \text{ fm}/c$). Although the jet source terms vanish before the

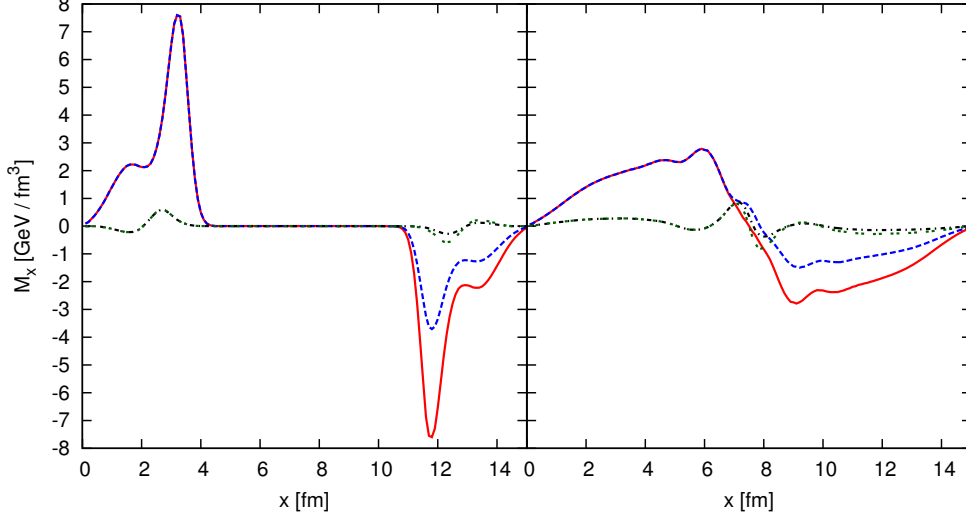


Figure 5. Momentum density along the trajectory of the jets in opposite directions. Left panel: momentum density at the moment of extinction. Right panel: momentum density after another 2.5 fm/c. Red solid line: pair of jets with equal energy. Blue dashed line: pair of jets where jet on the right has originally a half of the other jet's energy. Green double dashed line: pair of jets in opposite directions, jet on the right is moving along the x-axis in the axial distance of 2 fm from the other jet's trajectory; momentum density distribution is taken along the line in centre between the two jets. Black dash and dotted line: same as previous case but jet entering from right has originally a half of the other jet's energy.

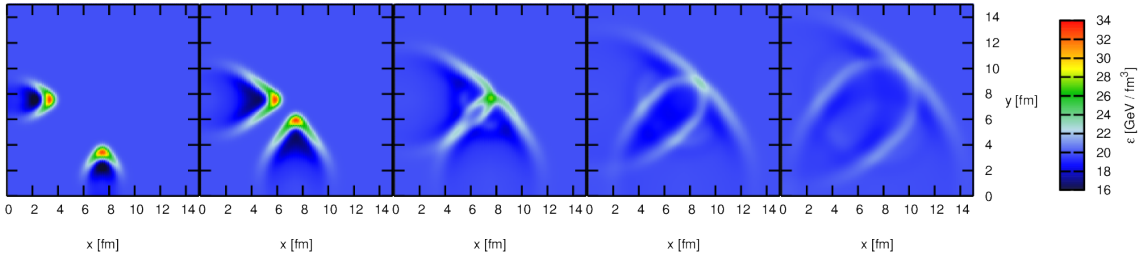


Figure 6. Sequence of energy density profiles during hydrodynamical evolution. Two hard partons deposit energy and momentum into static medium. One enters from the left, one enters from the bottom. First profile is taken after a delay of $t = 2.5$ fm/c, the subsequent profiles after time steps $\Delta t = 2.5$ fm/c. Jets are fully quenched after 5 fm/c. The initial energy loss is $dE/dx = -8.296$ GeV/fm, initial velocity is $v_{jet} = 0.9999$, unperturbed static energy density is $\epsilon_0 = 20$ GeV/fm³.

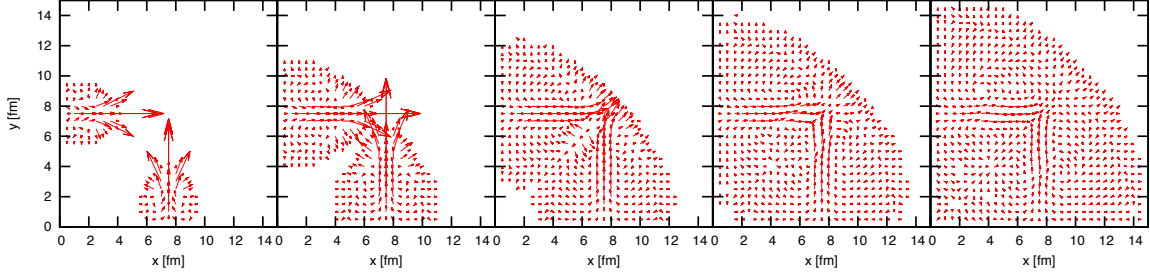


Figure 7. Situation from Fig. 6. The direction and length of arrows correspond to the direction and magnitude of local momentum density, respectively.

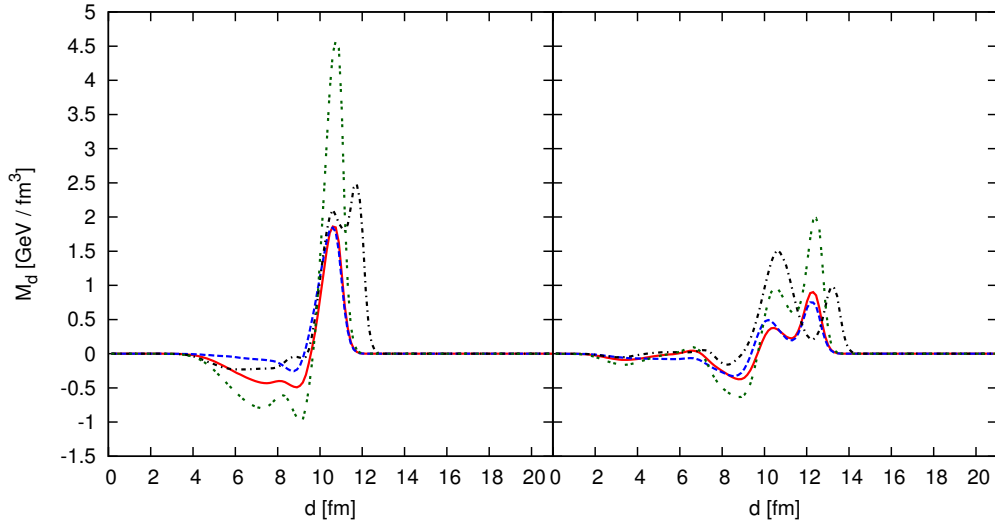


Figure 8. Momentum density in diagonal direction during hydrodynamic evolution as a function of the diagonal coordinate. Jets move perpendicularly to each other and source terms vanish at $t = 5 \text{ fm}/c$, which is $1.5 \text{ fm}/c$ before they would meet, unless stated otherwise. Left panel: profile at $t = 7.5 \text{ fm}/c$, right panel: $t = 10.0 \text{ fm}/c$. Red solid line: perpendicular jets scenario, both jets have equal energy. Blue dashed line: same scenario as before but the lower side jet has a half of the other jet's energy. Green double dashed line: each jet deposits two times more energy than in the first case. Black dash and dotted line: jets source terms vanish only $0.5 \text{ fm}/c$ before jets would meet.

wakes make contact, the merged wakes continue to evolve. Momentum density also exhibits double peak structure. Behind the merged wakes the momentum density turns negative, i.e. it points backwards. This is a part of the vortices that are built up on the sides around the jets. We observe that the lower unperturbed energy density or higher

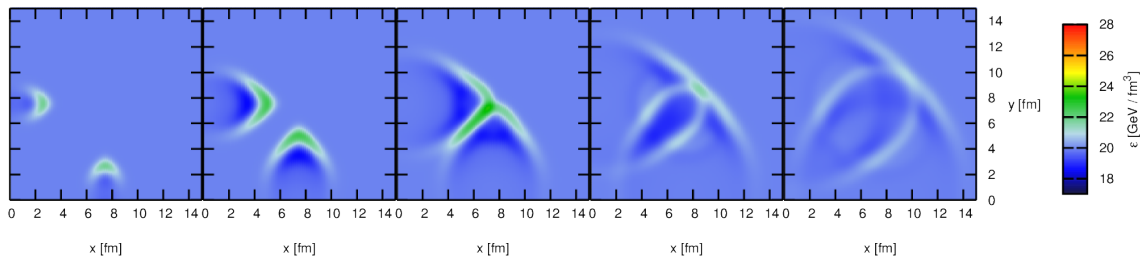


Figure 9. Sequence of energy density profiles during a hydrodynamical evolution. Two hard partons deposit energy and momentum into static medium. One enters from the left, one enters from the bottom. Distance of closest approach of extrapolated trajectories is 2 fm. Profiles are taken on the plane in the middle of both trajectories. First profile is taken after $t = 2.5$ fm/ c . All other profiles are taken with subsequent delays $\Delta t = 2.5$ fm/ c . Jets are quenched after 5 fm/ c , i.e. in the second figure. The initial energy loss is $dE/dx = -4.148$ GeV/fm, initial velocity is $v_{jet} = 0.9999$, unperturbed static energy density is $\epsilon_0 = 20$ GeV/fm³.

energy-momentum deposition induce higher momentum density on the diagonal when wakes merge, as expected. The peaks in momentum density corresponding to merging of two wakes with equal and also with unequal energy seem qualitatively similar.

It is very rare, however, that two jets would be aimed so precisely that their wakes meet exactly as it was assumed here. Therefore, we examine a situation with velocities perpendicular to each other but the distance of closest approach of their extrapolated trajectories is 2 fm. The evolution of the energy density on the plane in the middle between the two trajectories is shown in Fig. 9. We checked also the plots of velocity and momentum densities. The wake streams and their merging is less visible in such a distance from the original jets. On the other hand, one better sees the vortices that are built at the two sides behind the jet.

Diagonal dependences of the momentum density look in this case qualitatively similarly as in Fig. 8, only the size of momentum densities is typically lower.

4. Summary and conclusions

We presented simulations of energy and momentum deposition from hard partons into hot deconfined matter and studied the response of the matter. The aim of this toy model simulation was to verify that the streams which are generated in the wakes indeed carry the deposited momentum. It remains to be checked to what extent this feature may be spoiled by introducing momentum transport parametrised by viscosity into the simulation [25]. Moreover, when two streams meet and are not being stimulated anymore by a hard parton, they merge into one stream which continues until it is tamed by diffusion. We thus confirmed the assumption made in [16] that the generated wakes interact and influence each other. That paper concluded that under such conditions

in heavy ion collisions isotropically produced hard partons generate interacting wakes which can lead to collective motion that exhibits elliptic flow correlated with the direction of the reaction plane. It was estimated to be on the level of one or two per cent there.

Hence, we see that we have identified a mechanism which generates anisotropic flow and consequently anisotropic particle production in ultrarelativistic nuclear collisions. Let us stress again the difference to the hydrodynamic scenario with hot spots in the initial conditions. That model takes into account that the initial energy density profile for hydrodynamic simulation changes event-by-event. In contrast to our model all features unique for a given event are specified in the initial conditions from which hydrodynamics based on energy-momentum conservation is started. In our case, energy and momentum is deposited into the medium *during* its evolution and not only at the beginning.

The influence of hard partons on flow anisotropies will show itself in various orders of particle production anisotropies. It remains to be studied, how big the effect is in realistic simulations reproducing the dynamics of the fireball. Also, inclusion of viscosity will weaken the influence of this effect, but quantitative details remain to be investigated. When analyzing precision data from LHC (and RHIC) it will be important, however, to take this effect into account if one wants to make quantitative statements about the transport properties of the hot deconfined matter.

Acknowledgements This work was partially supported by RVO68407700 (Czech Republic). BT also acknowledges support by VEGA 1/0457/12 and APVV-0050-11 (Slovakia).

References

- [1] A. Accardi *et al.*, *Hard probes in heavy ion collisions at the LHC, Chapter 2: Jet physics*, CERN Yellow Report CERN-2004-009, hep-ph/0310274.
- [2] M. Gyulassy, D. H. Rischke and B. Zhang, Nucl. Phys. A **613** (1997) 397 [nucl-th/9609030].
- [3] O. Socolowski, Jr., F. Grassi, Y. Hama and T. Kodama, Phys. Rev. Lett. **93** (2004) 182301 [hep-ph/0405181].
- [4] R. P. G. Andrade, F. Grassi, Y. Hama, T. Kodama and W. L. Qian, Phys. Rev. Lett. **101**, 112301 (2008) [arXiv:0805.0018 [hep-ph]].
- [5] H. Petersen and M. Bleicher, Phys. Rev. C **79** (2009) 054904 [arXiv:0901.3821 [nucl-th]].
- [6] H. Petersen, C. Coleman-Smith, S. A. Bass and R. Wolpert, J. Phys. G **38** (2011) 045102 [arXiv:1012.4629 [nucl-th]].
- [7] H. Holopainen, H. Niemi and K. J. Eskola, Phys. Rev. C **83** (2011) 034901 [arXiv:1007.0368 [hep-ph]].
- [8] B. Schenke, S. Jeon and C. Gale, Phys. Rev. C **85** (2012) 024901 [arXiv:1109.6289 [hep-ph]].
- [9] Z. Qiu and U. W. Heinz, Phys. Rev. C **84** (2011) 024911 [arXiv:1104.0650 [nucl-th]].
- [10] F. G. Gardim, F. Grassi, M. Luzum and J. -Y. Ollitrault, Phys. Rev. Lett. **109** (2012) 202302 [arXiv:1203.2882 [nucl-th]].
- [11] P. Bozek and W. Broniowski, Phys. Rev. C **85** (2012) 044910 [arXiv:1203.1810 [nucl-th]].
- [12] S. Florschinger and U. A. Wiedemann, JHEP **1111** (2011) 100 [arXiv:1108.5535 [nucl-th]].

- [13] B. Betz, J. Noronha, G. Torrieri, M. Gyulassy, I. Mishustin and D. H. Rischke, *Phys. Rev. C* **79** (2009) 034902 [arXiv:0812.4401 [nucl-th]].
- [14] B. Betz, J. Noronha, G. Torrieri, M. Gyulassy and D. H. Rischke, *Phys. Rev. Lett.* **105** (2010) 222301 [arXiv:1005.5461 [nucl-th]].
- [15] B. Betz, *EPJ Web Conf.* **13** (2011) 07002 [arXiv:1012.4418 [nucl-th]].
- [16] B. Tomášik and P. Lévai, *J. Phys. G* **38** (2011) 095101 [arXiv:1104.3262 [nucl-th]].
- [17] L. M. Satarov, H. Stoecker and I. N. Mishustin, *Phys. Lett. B* **627** (2005) 64 [arXiv:hep-ph/0505245].
- [18] J. Casalderrey-Solana, E. V. Shuryak and D. Teaney, *J. Phys. Conf. Ser.* **27** (2005) 22 [Nucl. Phys. A **774** (2006) 577] [arXiv:hep-ph/0411315].
- [19] V. Koch, A. Majumder and X. N. Wang, *Phys. Rev. Lett.* **96** (2006) 172302 [arXiv:nucl-th/0507063].
- [20] J. Ruppert and B. Müller, *Phys. Lett. B* **618** (2005) 123 [arXiv:hep-ph/0503158].
- [21] T. Renk and J. Ruppert, *Phys. Rev. C* **73** (2006) 011901 [arXiv:hep-ph/0509036].
- [22] R. B. Neufeld, *Phys. Rev. D* **78** (2008) 085015 [arXiv:0805.0385 [hep-ph]].
- [23] R. B. Neufeld and T. Renk, *Phys. Rev. C* **82** (2010) 044903 [arXiv:1001.5068 [nucl-th]].
- [24] E. Shuryak, arXiv:1101.4839 [hep-ph].
- [25] I. Bouras, A. El, O. Fochler, H. Niemi, Z. Xu and C. Greiner, *Phys. Lett. B* **710** (2012) 641 [arXiv:1201.5005 [nucl-th]].
- [26] M. Laine, Y. Schroder, *Phys. Rev. D* **73**, (2006) 085009.
- [27] J. J. Friess, S. S. Gubser, G. Michalogiorgakis and S. S. Pufu, *Phys. Rev. D* **75**, 106003 (2007).
- [28] S. S. Gubser and A. Yarom, *Phys. Rev. D* **77**, 066007 (2008).
- [29] P. M. Chesler and L. G. Yaffe, *Phys. Rev. D* **78**, 045013 (2008).
- [30] T. Renk, *Phys. Rev. C* **85**, 044903 (2012).
- [31] T. Renk, H. Holopainen, R. Paatelainen and K. J. Eskola, *Phys. Rev. C* **84**, 014906 (2011).
- [32] H. Bethe, *Annalen der Physik* **397**, 325 (1930).
- [33] W. H. Bragg, R. Kleemann, *Philos. Mag.* **10**, (1905) 318.
- [34] J. P. Boris, D. L. Book, *J. Comp. Phys.* **11**, 38 (1973).
- [35] C. R. DeVore, *J. Comput. Phys.* **92**, 142 (1991).
- [36] S. T. Zalesak, *J. Comp. Phys.* **31**, 38 (1979).